Study on Numerical Methods for Gas Flow Simulation Using Double-Porosity Double-Permeability Model

Yi Wang[1[0000-0002-6294-1290]], Shuyu Sun[2[0000-0002-3078-864X]], Liang Gong[3]

[1] National Engineering Laboratory for Pipeline Safety/MOE Key Laboratory of Petroleum Engineering/Beijing Key Laboratory of Urban Oil and Gas Distribution Technology, China University of Petroleum (Beijing), Beijing 102249, China
[2] Computational Transport Phenomena Laboratory, Division of Physical Science and Engineering, King Abdullah University of Science and Technology, Thuwal 23955-6900, Saudi Arabia
[3] Department of Thermal Energy and Power Engineering, College of Pipeline and Civil Engineering, China University of Petroleum (Qingdao), Qingdao, Shandong 266580, China
wangyi1031@cup.edu.cn

Abstract. In this paper, we firstly study numerical methods for gas flow simulation in dual-continuum porous media. Typical methods for oil flow simulation in dual-continuum porous media cannot be used straightforward to this kind of simulation due to the artificial mass loss caused by the compressibility and the non-robustness caused by the non-linear source term. To avoid these two problems, corrected numerical methods are proposed using mass balance equations and local linearization of the non-linear source term. The improved numerical methods are successful for the computation of gas flow in the double-porosity double-permeability porous media. After this improvement, temporal advancement for each time step includes three fractional steps: i) advance matrix pressure and fracture pressure using the typical computation; ii) solve the mass balance equation system for mean pressures; iii) correct pressures in i) by mean pressures in ii). Numerical results show that mass conservation of gas for the whole domain is guaranteed while the numerical computation is robust.

Keywords: Mass conservation; Numerical method; Double-porosity double-permeability; Fractured porous media; Gas flow.

1 Introduction

Fractured reservoirs contain significant proportion of oil and gas reserves all over the world. This proportion is estimated to be over 20% for oil reserves [1] and probably higher for gas reserves [2]. The large proportion of petroleum in fractured reservoirs is a good supplementary to convectional petroleum resource, which cannot solely satisfy energy demands all over the world for oil and gas. Fractured reservoirs are

attracting petroleum industry and getting more developments. Despite well understandings and technological accumulations for conventional oil and gas, technologies for explorations in fractured reservoirs are relative immature due to the complicated structures and flow behaviors in fractured reservoirs. Therefore, researches driven by the increasing needs to develop petroleum in fractured reservoirs have been received growing attentions. Efforts on modeling and understanding the flow characteristics in fractured reservoirs have been made continuously [3]. Among the commonly used conceptual models, the double-porosity double-permeability model is probably widely used in petroleum engineering due to its good ability to match many types of laboratory or field data and has been utilized in commercial software [4].

Some numerical simulations [5] and analytical solutions [6,7] have been proposed for oil flow in dual-continuum porous media. However, analytical solutions can only be obtained under much idealized assumptions, such that slight compressibility, infinite radial flow, homogenization etc., so that their applications are restricted to simplified cases of oil flow. For gas flow, slight compressibility assumption is not held any more. The governing equations are nonlinear and cannot be analytically solved. Numerical computations for gas flow in dual-continuum porous media might be more difficult than oil flow because the strong nonlinearity induced by compressibility of gas. Therefore, it is important to study numerical methods for gas flow in fractured reservoirs based on the dual-continuum model. We also numerically study the effect of the production well on the gas production in a dual-continuum porous medium with non-uniform fracture distribution.

2 Governing equations and numerical methods

2.1 Physical model and governing equations

Fig.1 shows the computational domain. The side length of the domain is L. Other sets can be found in the figure.

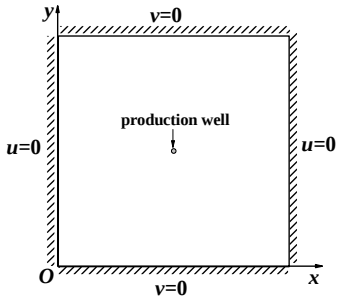

Fig. 1. Physical model

Darcy's law in a dual-continuum system is:

$$u_M = -\frac{k_{xxM}}{\mu}\frac{\partial p_M}{\partial x}, v_M = -\frac{k_{yyM}}{\mu}\frac{\partial p_M}{\partial y} \tag{1}$$

$$u_F = -\frac{k_{xxF}}{\mu}\frac{\partial p_F}{\partial x}, v_F = -\frac{k_{yyF}}{\mu}\frac{\partial p_F}{\partial y} \tag{2}$$

where u_M and v_M are two components of Darcy velocity of gas flow in matrix, u_F and v_F are two components of Darcy velocity of gas flow in fracture, k_{xxM} and k_{yyM} are two components of matrix permeability, k_{xxF} and k_{yyF} are two components of fracture permeability, p_M and p_F are pressures in matrix and fracture respectively. μ is the dynamic viscosity.

Mass conservation equations for gas flow in dual-continuum reservoirs governed by Darcy's law are:

$$\phi_M \frac{\partial p_M}{\partial t} = \frac{\partial}{\partial x}\left(\frac{k_{xxM}}{\mu} p_M \frac{\partial p_M}{\partial x}\right) + \frac{\partial}{\partial y}\left(\frac{k_{yyM}}{\mu} p_M \frac{\partial p_M}{\partial y}\right) - \alpha \frac{k_M}{\mu} p_M \left(p_M - p_F\right) \tag{3}$$

$$\phi_F \frac{\partial p_F}{\partial t} = \frac{\partial}{\partial x}\left(\frac{k_{xxF}}{\mu} p_F \frac{\partial p_F}{\partial x}\right) + \frac{\partial}{\partial y}\left(\frac{k_{yyF}}{\mu} p_F \frac{\partial p_F}{\partial y}\right) + \alpha \frac{k_M}{\mu} p_M \left(p_M - p_F\right) - \delta_w C_w p_F \left(p_F - p_{bh}\right) \tag{4}$$

Where ϕ_M and ϕ_F are porosities of matrix and fracture respectively, k_M is the intrinsic permeability of matrix for the matrix-fracture interaction term. α is the shape factor of fracture, taking the form proposed by Kazemi et al. [8]:

$$\alpha = 4\left(\frac{1}{l_x^2} + \frac{1}{l_y^2}\right) \tag{5}$$

Where l_x and l_y are the lengths of fracture spacing in the *x* and *y* directions respectively. C_w is a factor of the well:

$$C_w = \frac{2\pi k_F}{\mu h_x h_y \ln\left(r_e / r_w\right)} \tag{6}$$

Where k_F is the permeability of fracture at the location of the production well, h_x and h_y are side lengths of the grid containing the well, r_w and r_e are well radius and equivalent radius ($r_e = 0.20788h$, $h = h_x = h_y$ and $h_x = \Delta x$, $h_y = \Delta y$ for uniform square grid). C_w is 1 for the grid cell containing the well and 0 for other cells. p_{bh} is the bottom hole pressure.

2.2 Numerical methods

The above governing equations are similar with those of oil flow in dual-continuum porous media so that we directly apply the numerical methods for oil flow to gas flow at first. Finite difference method is used on staggered grid. Temporal advancement is the semi-implicit scheme to ensure a large time step. Spatial discretization adopts the second-order central difference scheme. Based on these methods, Eq.(3) and Eq.(4) are discretized to:

$$cp_{Mi,j} p_{Mi,j}^{(n+1)} = cex_{Mi,j} p_{Mi+1,j}^{(n+1)} + cwx_{Mi,j} p_{Mi-1,j}^{(n+1)} + cny_{Mi,j} p_{Mi,j+1}^{(n+1)} + csy_{Mi,j} p_{Mi,j-1}^{(n+1)} + b_{Mi,j} \tag{7}$$

$$\left(cp_{Fi,j}+\delta_w C_w \Delta t\left(p_{Fi,j}^{(n)}-p_{bh}\right)\right)p_{Fi,j}^{(n+1)}-\Delta t\frac{\alpha k_{Mi,j}}{\mu}p_{Mi,j}^{(n)}p_{Mi,j}^{(n+1)} \tag{8}$$
$$=cex_{Fi,j}p_{Fi+1,j}^{(n+1)}+cwx_{Fi,j}p_{Fi-1,j}^{(n+1)}+cny_{Fi,j}p_{Fi,j+1}^{(n+1)}+csy_{Fi,j}p_{Fi,j-1}^{(n+1)}+b_{Fi,j}$$

Where $cp_{Mi,j}=\phi_M+cwx_{Mi,j}+cex_{Mi,j}+csy_{Mi,j}+cny_{Mi,j}+\Delta t\frac{\alpha k_{Mi,j}}{\mu}p_{Mi,j}^{(n)}\left(1-\frac{p_{Fi,j}^{(n)}}{p_{Mi,j}^{(n)}}\right)$,

$cp_{Fi,j}=\phi_F+cwx_{Fi,j}+cex_{Fi,j}+csy_{Fi,j}+cny_{Fi,j}+\Delta t\frac{\alpha k_{Mi,j}}{\mu}p_{Mi,j}^{(n)}$,

$b_{Mi,j}=\phi_M p_{Mi,j}^{(n)}+swx_{Mi,j}+sex_{Mi,j}+ssy_{Mi,j}+sny_{Mi,j}$,

$b_{Fi,j}=\phi_F p_{Fi,j}^{(n)}+swx_{Fi,j}+sex_{Fi,j}+ssy_{Fi,j}+sny_{Fi,j}$. Other coefficients are not shown here due to the limitation of the paper.

3 Discussions on numerical method

The discretized equations are solved using parameters in Table 1. Computational results show that the well pressure is always negative, which is unphysical, because all pressures must be higher than P_{bh} (2atm). We further find the difference between initial total mass and computational total mass is increasing (Fig.2), indicating that gas mass is lost in the computation. This phenomenon demonstrates that current numerical methods cannot automatically ensure the mass conservation, although the computation is based on the mass conservation equation (Eq.(3) and Eq.(4)). Therefore, mass conservation law should be utilized to correct current numerical methods.

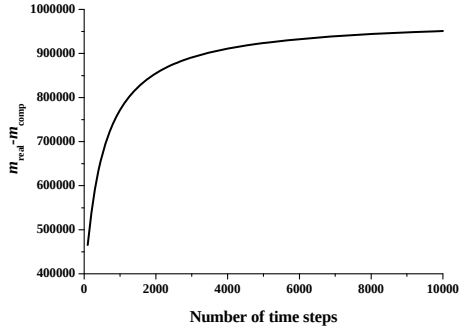

Fig. 2. Difference between real mass and computational mass

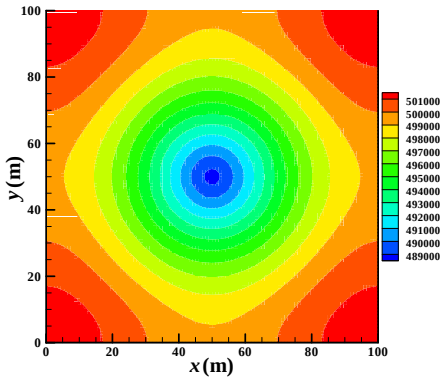

Fig. 3. Matrix pressure after 10000 Δt

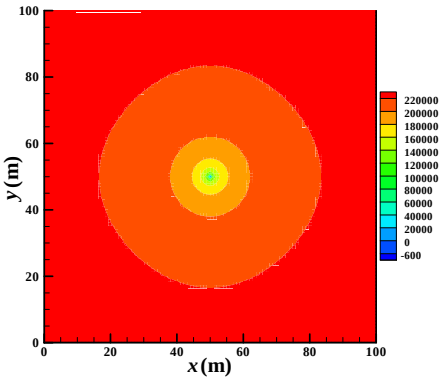

Fig. 4. Fracture pressure after 10000 Δt

Table 1. Computational parameters

Parameter	Value	Unit
ϕ_M	0.5	/
ϕ_F	0.001	/
$p_M(t_0)$	100	atm
$p_F(t_0)$	100	atm
p_{bh}	2	atm
k_{xxF}	100	md
k_{yyF}	100	md
k_{xxM}	1	md
k_{yyM}	1	md
k_M	1	md
W	16	g/mol
R	8.3147295	J/(mol·K)
T	25	^oC
μ	11.067×10^{-6}	Pa·s
nx	101	/
ny	101	/
L	100	m
l_x	20	cm
l_y	20	cm
r_w	20	cm
Δt	0.24	h

*1atm=101325Pa; 1md=$9.8692327\times10^{-16}m^2$; t_0 represents initial time.

Matrix pressure and fracture pressure at $10000\Delta t$ are shown in Fig.3 and Fig.4 respectively. Their distributions indicate that pressure gradients are correct. Thus, the incorrect pressures are caused by the unreal mean pressures. They can be corrected by the real mean pressures as follows:

$$\left(p_M^{(n+1)}\right)_{i,j} = \left(p_M^*\right)_{i,j} - \overline{p_M^*} + \overline{p_M^{real}} \tag{9}$$

$$\left(p_F^{(n+1)}\right)_{i,j} = \left(p_F^*\right)_{i,j} - \overline{p_F^*} + \overline{p_F^{real}} \tag{10}$$

Where $\left(p_M^{(n+1)}\right)_{i,j}$ and $\left(p_F^{(n+1)}\right)_{i,j}$ are the corrected matrix pressure and fracture pressure to be solved, $\left(p_M^*\right)_{i,j}$ and $\left(p_F^*\right)_{i,j}$ are the uncorrected matrix pressure and fracture pressure obtained from the numerical methods in Section 2.2, $\overline{p_M^*}$ and $\overline{p_F^*}$ are the unreal mean pressures of matrix and pressure calculated from $\left(p_M^*\right)_{i,j}$ and $\left(p_F^*\right)_{i,j}$, $\overline{p_M^{real}}$ and $\overline{p_F^{real}}$ are the real mean pressures of matrix and fracture which are unknown because they are dependent on $\left(p_M^{(n+1)}\right)_{i,j}$ and $\left(p_F^{(n+1)}\right)_{i,j}$. $\left(p_M^*\right)_{i,j}$, $\left(p_F^*\right)_{i,j}$, $\overline{p_M^*}$ and $\overline{p_F^*}$ can be calculated via the numerical methods in Section 2.2 so that they are all known variables for each time step. Thus, the calculation of $\left(p_M^{(n+1)}\right)_{i,j}$ and $\left(p_F^{(n+1)}\right)_{i,j}$ turns to the calculation of unknown $\overline{p_M^{real}}$ and $\overline{p_F^{real}}$. Gas is continuously flowing from matrix to fracture and leaving the dual-continuum system from the well. Therefore, mass balance of matrix in each time step should be:

$$mM^{(n)} - mT^{(n+1)} = mM^{(n+1)} \tag{11}$$

Mass balance of fracture in each time step is:

$$mF^{(n)} + mT^{(n+1)} - Q^{(n+1)} = mF^{(n+1)} \tag{12}$$

Where $mM^{(n)}$ and $mF^{(n)}$ are the masses of gas in matrix and fracture at the beginning moment of each time step, $mM^{(n+1)}$ and $mF^{(n+1)}$ are the masses of gas in matrix and fracture at the ending moment of each time step, $mT^{(n+1)}$ is the mass leaving matrix (i.e. equivalent to the mass entering fracture) at each time step, $Q^{(n+1)}$ is the mass leaving the fracture via the production well at each time step.

Eq.(3) and Eq.(4) are mass conservation equations in the unit of Pa/s. $\Delta x\Delta y\Delta t\dfrac{W}{RT}$ should be multiplied to all terms of Eq.(3) and Eq.(4) to obtain the masses in Eq.(11) and Eq.(12):

$$mT^{(n+1)} = \Delta x\Delta y\Delta t\frac{W}{RT}\sum_{j=1}^{ny}\sum_{i=1}^{nx}\left[\alpha\left(\frac{k_M}{\mu}\right)_{i,j}\left(p_M^{(n+1)}\right)_{i,j}\left(\left(p_M^{(n+1)}\right)_{i,j} - \left(p_F^{(n+1)}\right)_{i,j}\right)\right] \tag{13}$$

$$Q^{(n+1)} = \Delta x \Delta y \Delta t \frac{W}{RT} \delta_w C_w p_F^{(n+1)} \left(p_F^{(n+1)} - p_{bh} \right) \tag{14}$$

The masses of gas can be calculated via equation of state:

$$mM^{(n+1)} = \sum_{j=1}^{ny} \sum_{i=1}^{nx} \left(p_M^{(n+1)} \right)_{i,j} \Delta x \Delta y \frac{W}{RT} \tag{15}$$

$$mF^{(n+1)} = \sum_{j=1}^{ny} \sum_{i=1}^{nx} \left(p_F^{(n+1)} \right)_{i,j} \Delta x \Delta y \frac{W}{RT} \tag{16}$$

$$mM^{(n)} = \sum_{j=1}^{ny} \sum_{i=1}^{nx} \left(p_M^{(n)} \right)_{i,j} \Delta x \Delta y \frac{W}{RT} \tag{17}$$

$$mF^{(n)} = \sum_{j=1}^{ny} \sum_{i=1}^{nx} \left(p_F^{(n)} \right)_{i,j} \Delta x \Delta y \frac{W}{RT} \tag{18}$$

Eq.(17) and Eq.(18) can be used to directly obtain the values of $mM^{(n)}$ and $mF^{(n)}$ in every time step. Eq.(13)~Eq.(16) are substituted to Eq.(11) and Eq.(12) so that the mass balance equations become:

$$\begin{aligned} & mM^{(n)} - \Delta x \Delta y \Delta t \frac{W}{RT} \sum_{j=1}^{ny} \sum_{i=1}^{nx} \left[\alpha \left(\frac{k_M}{\mu} \right)_{i,j} \left(p_M^{(n+1)} \right)_{i,j} \left(\left(p_M^{(n+1)} \right)_{i,j} - \left(p_F^{(n+1)} \right)_{i,j} \right) \right] \\ & = \sum_{j=1}^{ny} \sum_{i=1}^{nx} \left(p_M^{(n+1)} \right)_{i,j} \Delta x \Delta y \frac{W}{RT} \end{aligned} \tag{19}$$

$$\begin{aligned} & mF^{(n)} + \Delta x \Delta y \Delta t \frac{W}{RT} \sum_{j=1}^{ny} \sum_{i=1}^{nx} \left[\alpha \left(\frac{k_M}{\mu} \right)_{i,j} \left(p_M^{(n+1)} \right)_{i,j} \left(\left(p_M^{(n+1)} \right)_{i,j} - \left(p_F^{(n+1)} \right)_{i,j} \right) \right] \\ & - \Delta x \Delta y \Delta t \frac{W}{RT} \delta_w C_w p_F^{(n+1)} \left(p_F^{(n+1)} - p_{bh} \right) = \sum_{j=1}^{ny} \sum_{i=1}^{nx} \left(p_F^{(n+1)} \right)_{i,j} \Delta x \Delta y \frac{W}{RT} \end{aligned} \tag{20}$$

Eq.(9) and Eq.(10) are substituted to the above two equations to obtain the following expressions:

$$\begin{aligned} & - \left[\alpha \Delta x \Delta y \Delta t \sum_{j=1}^{ny} \sum_{i=1}^{nx} \left(\frac{k_M}{\mu} \right)_{i,j} \right] \left(\overline{p_M^{real}} \right)^2 + \left[\alpha \Delta x \Delta y \Delta t \sum_{j=1}^{ny} \sum_{i=1}^{nx} \left(\frac{k_M}{\mu} \right)_{i,j} \right] \overline{p_M^{real}} \, \overline{p_F^{real}} \\ & - \left[L_x L_y + \alpha \Delta x \Delta y \Delta t \sum_{j=1}^{ny} \sum_{i=1}^{nx} \left(\frac{k_M}{\mu} \right)_{i,j} \left(2 \left(p_M^* \right)_{i,j} - 2 \overline{p_m^*} - \left(p_F^* \right)_{i,j} + \overline{p_F^*} \right) \right] \overline{p_M^{real}} \\ & + \left[\alpha \Delta x \Delta y \Delta t \sum_{j=1}^{ny} \sum_{i=1}^{nx} \left(\frac{k_M}{\mu} \right)_{i,j} \left(\left(p_M^* \right)_{i,j} - \overline{p_M^*} \right) \right] \overline{p_F^{real}} \\ & - \alpha \Delta x \Delta y \Delta t \sum_{j=1}^{ny} \sum_{i=1}^{nx} \left(\frac{k_M}{\mu} \right)_{i,j} \left(\left(p_M^* \right)_{i,j} - \overline{p_M^*} \right) \left(\left(p_M^* \right)_{i,j} - \overline{p_M^*} - \left(p_F^* \right)_{i,j} + \overline{p_F^*} \right) + mM^{(n)} \frac{RT}{W} = 0 \end{aligned} \tag{21}$$

$$
\begin{aligned}
&\left[\alpha\Delta x\Delta y\Delta t\sum_{j=1}^{ny}\sum_{i=1}^{nx}\left(\frac{k_M}{\mu}\right)_{i,j}\right]\left(\overline{p_M^{real}}\right)^2-C_w\Delta x\Delta y\Delta t\left(\overline{p_F^{real}}\right)^2-\left[\alpha\Delta x\Delta y\Delta t\sum_{j=1}^{ny}\sum_{i=1}^{nx}\left(\frac{k_M}{\mu}\right)_{i,j}\right]\overline{p_M^{real}}\,\overline{p_F^{real}}\\
&+\left[\alpha\Delta x\Delta y\Delta t\sum_{j=1}^{ny}\sum_{i=1}^{nx}\left(\frac{k_M}{\mu}\right)_{i,j}\left(2\left(p_M^*\right)_{i,j}-2\overline{p_M^*}-\left(p_F^*\right)_{i,j}+\overline{p_F^*}\right)\right]\overline{p_M^{real}}\\
&-\left[L_xL_y+\alpha\Delta x\Delta y\Delta t\sum_{j=1}^{ny}\sum_{i=1}^{nx}\left(\frac{k_M}{\mu}\right)_{i,j}\left(\left(p_M^*\right)_{i,j}-\overline{p_M^*}\right)+C_w\Delta x\Delta y\Delta t\left(2\left(p_F^*\right)_{iW,jW}-2\overline{p_F^*}-p_{bh}\right)\right]\overline{p_F^{real}} \qquad (22)\\
&+\alpha\Delta x\Delta y\Delta t\sum_{j=1}^{ny}\sum_{i=1}^{nx}\left(\frac{k_M}{\mu}\right)_{i,j}\left(\left(p_M^*\right)_{i,j}-\overline{p_M^*}\right)\left(\left(p_M^*\right)_{i,j}-\overline{p_M^*}-\left(p_F^*\right)_{i,j}+\overline{p_F^*}\right)\\
&-C_w\Delta x\Delta y\Delta t\left(\left(p_F^*\right)_{iW,jW}-\overline{p_F^*}\right)\left(\left(p_F^*\right)_{iW,jW}-\overline{p_F^*}-p_{bh}\right)+mF^{(n)}\frac{RT}{W}=0
\end{aligned}
$$

where *iW*, *jW* are the grid numbers of the well in the *x* and *y* directions respectively. Eq.(21) and Eq.(22) are the final expressions of mass balance equations Eq.(11) and Eq.(12). $\overline{p_M^{real}}$ and $\overline{p_F^{real}}$ can be directly solved combining these two equations. Once the combined equations (Eq.(21) and Eq.(22)) are solved, $\overline{p_M^{real}}$ and $\overline{p_F^{real}}$ are obtained so that pressures can be corrected using Eq.(9) and Eq.(10) for every time step.

Table 2. Well pressure and mass difference after improvement

n_t/100	1	2	3	…	10	11	12	13	14
p_{well}	3.83	3.63	3.47	…	2.80	2.74	2.69	2.65	2.75
m_{real}-m_{comp}	0	0	0	…	0	0	0	0	0

Well pressure and total mass of gas using the above method considering mass conservation law are shown in Table 2. Well pressure becomes positive. The mass difference is always zero to show the mass conservation is satisfied. However, the well pressure (p_{well}) in Table 2 has an unphysical inverse. This is due to the diagonal dominance cannot be satisfied. It is clear in the governing equations that only the well term $\delta_w C_w\Delta t\left(p_{Fi,j}^{(n)}-p_{bh}\right)$ may cause the diagonal coefficient decreasing. Thus, the nonlinear well term ($S=-\delta_w C_w p_F\left(p_F-p_{bh}\right)$) in Eq.(4) should be transformed to the form of $S=S_c+S_p p_F$ with $S_p\le 0$ [9]. S_c and S_p can be obtained by the following Taylor expansion:

$$
\begin{aligned}
S&=S^{(n)}+\left.\frac{dS}{dp_F}\right|^{(n)}\left(p_F^{(n+1)}-p_F^{(n)}\right)\\
&=-\delta_w C_w p_F^{(n)}\left(p_F^{(n)}-p_{bh}\right)-\delta_w C_w\left(2p_F^{(n)}-p_{bh}\right)\left(p_F^{(n+1)}-p_F^{(n)}\right)\\
&=\delta_w C_w p_F^{(n)2}-\delta_w C_w\left(2p_F^{(n)}-p_{bh}\right)p_F^{(n+1)}
\end{aligned}
\qquad (23)
$$

Eq.(23) is used in the discretization of Eq.(4) instead of $S=-\delta_w C_w p_F\left(p_F-p_{bh}\right)$ so that Eq.(8) can be modified to be the following form:

$$\begin{aligned}&\left(cp_{Fi,j}+\delta_w C_w \Delta t\left(2p_{Fi,j}^{(n)}-p_{bh}\right)\right)p_{Fi,j}^{(n+1)}-\Delta t\frac{\alpha k_{Mi,j}}{\mu}p_{Mi,j}^{(n)}p_{Mi,j}^{(n+1)}\\&=cex_{Fi,j}p_{Fi+1,j}^{(n+1)}+cwx_{Fi,j}p_{Fi-1,j}^{(n+1)}+cny_{Fi,j}p_{Fi,j+1}^{(n+1)}+csy_{Fi,j}p_{Fi,j-1}^{(n+1)}+b_{Fi,j}+\delta_w C_w p_F^{(n)2}\end{aligned} \tag{24}$$

Fig.5 shows that p_{well} decreases monotonically and is always larger than p_{bh} after this improvement.

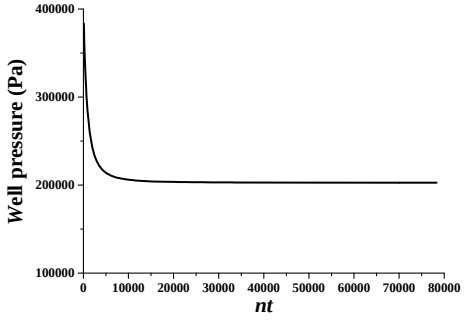

Fig. 5. Improved well pressure using linearization of source term

4 Conclusion

From the above discussions, the proposed numerical methods can be summarized as follows: 1) Governing equations should be discretized into the form of Eq.(7) and Eq.(24) respectively, using linearization of source term; 2) Mass conservation equation (Eq.(21) and Eq.(22)) should be established according to the mass balance of the whole system and solved to obtain real mean pressures of matrix and fracture in every time step; 3) Matrix pressure and fracture pressure should be corrected using the mean pressures obtained in 2). Future computations could be made using field data in engineering.

Acknowledgements

The work presented in this paper has been supported by National Natural Science Foundation of China (NSFC) (No.51576210, No.51676208), Science Foundation of China University of Petroleum-Beijing (No.2462015BJB03), and also supported in part by funding from King Abdullah University of Science and Technology (KAUST) through the grant BAS/1/1351-01-01.

References

1. Firoozabadi, A.: Recovery mechanisms in fractured reservoirs and field performance. J. Can. Petrol. Technol. 39, 13-17 (2000).
2. Bourbiaux, B.: Fractured reservoir simulation: a challenging and rewarding issue. Oil Gas Sci. Technol. 65, 227-238 (2010).
3. Wu, Y.S., Di, Y., Kang, Z., Fakcharoenphol, P.: A multiple-continuum model for simulating single-phase and multiphase flow in naturally fractured vuggy reservoirs. J. Pet. Sci. Eng. 78, 13-22 (2011).
4. Wu, Y.S., Lu, G., Zhang, K., Pan, L., Bodvarsson, G.S.: Analyzing unsaturated flow patterns in fractured rock using an integrated modeling approach. Hydrogeol. J. 15, 553-572 (2007).
5. Presho, M., Wo, S., Ginting, V.: Calibrated dual porosity dual permeability modeling of fractured reservoirs. J. Pet. Sci. Eng. 77, 326-337 (2011).
6. Huang, C.S., Chen, Y.L., Yeh, H.D.: A general analytical solution for flow to a single horizontal well by Fourier and Laplace transforms. Adv. Water Resour. 34, 640-648 (2011).
7. Nie, R.S., Meng, Y.F., Jia, Y.L., Zhang, F.X., Yang, X.T., Niu, X.N.: Dual porosity and dual permeability modeling of horizontal well in naturally fractured reservoir. Transp. Porous Media 92, 213-235 (2012).
8. Kazemi, H., Merrill, L.S., Porterfield, K.L., Zeman, P.R.: Numerical simulation of water-oil flow in naturally fractured reservoirs. SPE J. 16, 317-326 (1976).
9. Tao, W.Q.: Numerical heat transfer. 2nd ed., Xi'an Jiaotong University Press, Xi'an, China (2002)